Chapter 26
MODIS Vegetation Indices

**Alfredo Huete, Kamel Didan, Willem van Leeuwen,
Tomoaki Miura, and Ed Glenn**

26.1   Introduction

Assessments of vegetation condition, cover, change, and processes are major
components of global change research programs, and are topics of considerable
societal relevance. Spectral vegetation indices are among the most widely used
satellite data products, which provide key measurements for climate, hydrologic,
and biogeochemical studies; phenology, land cover, and land cover change detec-
tion; natural resource management and sustainable development. Vegetation indices
(VI) are robust and seamless data products computed similarly across all pixels in
time and space, regardless of biome type, land cover condition, and soil type, and
thus represent true surface measurements. The simplicity of VIs enables their amal-
gamation across sensor systems, which facilitates an ensured continuity of critical
datasets for long-term land surface modeling and climate change studies. Currently,
a more than two decades long NOAA Advanced Very High Resolution Radiometer
(AVHRR)-derived consistent global normalized difference vegetation index (NDVI)
land record exists, which has contributed significantly to global biome, ecosystem,
and agricultural studies.

In this chapter, we present the current status of the Moderate Resolution Imaging
Spectroradiometer (MODIS) VI products, their algorithm state and heritage,
validation, and QA. We highlight some important advances in land remote sensing
science, and discuss the full range of applications and societal benefits resulting from
the use of MODIS VIs.

A. Huete (✉)
Department Soil, Water & Environmental Science,
University of Arizona, Tucson, AZ 85721, USA
e-mail: ahuete@Ag.arizona.edu

26.2   Definition and Theoretical Basis

Vegetation indices are optical measures of vegetation canopy "greenness," a *composite* property of leaf chlorophyll, leaf area, canopy cover, and structure. VIs are not "intrinsic physical quantities" but are widely used as proxies to assess canopy biophysical/biochemical variables (leaf area index (LAI), fraction of absorbed photosynthetically active radiation (fPAR), chlorophyll content, green vegetation fraction (Fg), biomass) and canopy biophysical processes (photosynthesis, transpiration) (Choudhury 1987; Tucker 1979). A VI combines the chlorophyll-absorbing red spectral region with the nonabsorbing leaf reflectance signal in the near-infrared (NIR) to depict vegetation "greenness" or area-averaged canopy photosynthetic capacity. A variety of ways exist in which the red and NIR bands are combined to estimate greenness, and this produces a multitude of VI equations, including band ratios and differences (Gallo and Eidenshink 1988), normalized differences (Tucker 1979), linear combinations, and "optimized" band combinations (Huete 1988; Gobron et al. 2000). All VIs are empirically related with various vegetation canopy properties; however, there are significant differences in how they depict "greenness" and multiple VIs are potentially useful and complementary.

The MODIS standard VI products include the NDVI and the enhanced vegetation index (EVI) to more effectively characterize vegetation states and processes, and to better encompass the range of biophysical/biochemical information extractable from vegetated surfaces. The NDVI is a functional variant of the simple ratio (SR = NIR/red) that provides VI values normalized between -1 and +1,

$$\text{NDVI} = (\text{SR}-1)/(\text{SR}+1) = (\rho_{\text{NIR}} - \rho_{\text{red}})/(\rho_{\text{NIR}} + \rho_{\text{red}}) \qquad (26.1)$$

Several recent advances in earth science, specific to the global biome and agricultural primary production are attributable to the development and consistency of the AVHRR-NDVI time-series since 1981. They include interannual fluctuations and impacts of El Niño-Southern Oscillation on primary production, phenology, and climate change and variability. The NDVI data record has played a key role in detecting changes in vegetation caused by global temperature increases (Tucker et al. 2005), such as lengthening of the growing season at northern latitudes in response to global temperature increases (Myneni et al. 1997). An important advantage of the NDVI as a ratio, is its ability to normalize and produce stable values across large variations in incoming direct/diffuse irradiances. However, this also results in some disadvantages including the nonlinear nature of ratios, sensitivity to soil background, and saturation at moderate-to-high vegetation densities (Jiang et al. 2006; Huete et al. 2002).

The EVI gains its heritage from the soil adjusted vegetation index (SAVI) and the atmospheric resistance vegetation index, and is an optimized combination of blue, red, and NIR bands, based on Beer's law of canopy radiative transfer, designed to extract canopy greenness, independent of the underlying soil background and atmospheric aerosol variations (Huete 1988; Kaufman and Tanré 1992),

$$EVI = 2.5(\rho_N - \rho_R) / (L + \rho_N + C_1\rho_R - C_2\rho_B) \qquad (26.2)$$

where $\rho_{N,R,B}$ are reflectances in the NIR, red, and blue bands, respectively; L is the canopy background adjustment factor (Huete 1989); and C_1 and C_2 are the aerosol resistance weights (Liu and Huete 1995). The coefficients of the MODIS EVI equation are $L = 1$; $C_1 = 6$, and $C_2 = 7.5$ (Huete et al. 2002).

The blue band in the EVI is primarily used to stabilize aerosol influences in the red band resulting from residual and aerosol miscorrection (Miura et al. 1998; Xiao et al. 2003). The NDVI is sensitive to the canopy-absorbing "red" band, and has a lower optical penetrating depth in canopies, and thus will saturate more quickly in high biomass areas. The EVI becomes increasingly sensitive to the NIR band at moderate-to-high vegetation amounts with a greater optical depth penetration into canopies. Thus, the EVI will better depict biophysical canopy structural variations, and is less prone to saturate in high biomass areas (Gao et al. 2000).
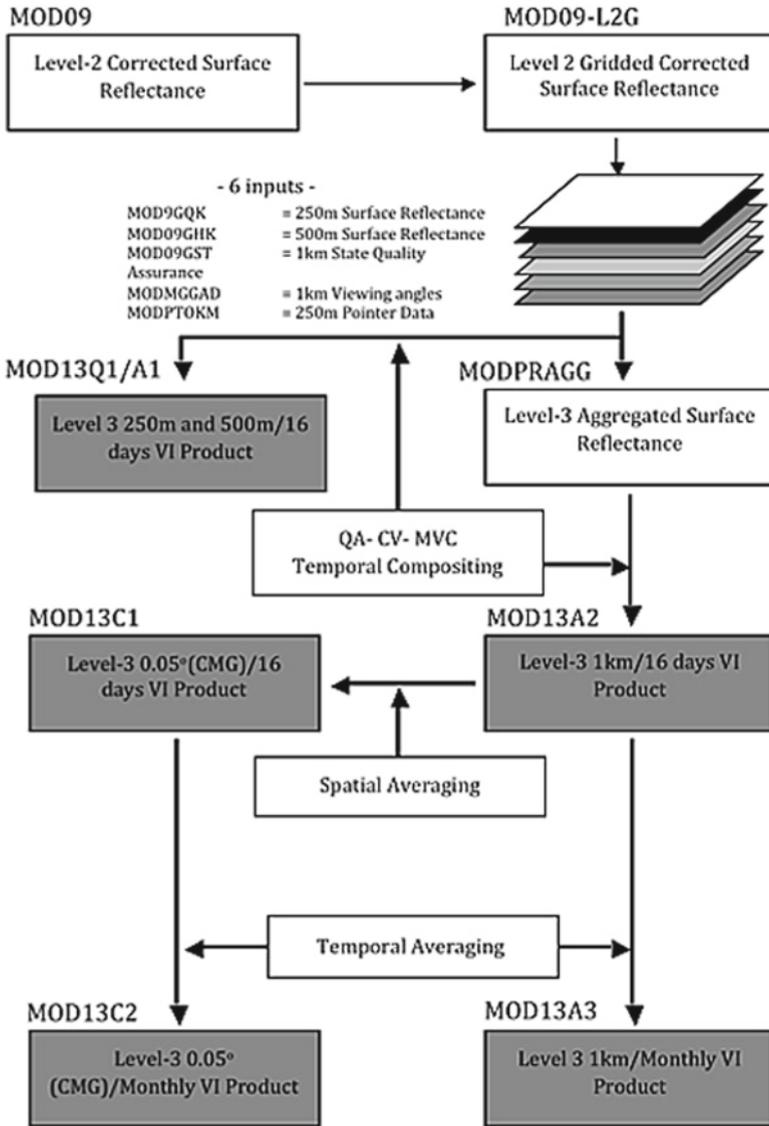
26.3 Algorithm State and Heritage

Six VI products exist for each of Terra and Aqua MODIS-derived sensors at varying spatial resolutions to best capture the important spatial and temporal complexities associated with vegetation dynamics, biogeochemical and hydrological processes (Table 26.1). This includes moderate resolution, 250 m, 500 m, and 1 km, and coarse resolution, 0.05° (~5.6 km Climate Modeling Grid, CMG) products generated each 16 days, while two standard calendar month products are also generated at 1 km and CMG resolutions to meet the needs of the research and application communities (Fig. 26.1). The products are generated globally over spatial units called tiles that are 10° × 10° (about 1,200 km × 1,200 km at the equator) in the equal-area Sinusoidal projection. No horizontal or vertical tile numbers exist in the global CMG product.

The MODIS science algorithms have undergone several improvements and modifications, including the VIs. The most recent revision, termed "Collection 5" (C5), incorporates changes to known issues and problems identified in the previous Collection 4 (C4). Each new collection supersedes the previous and initiates a complete reprocessing of all MODIS land data products from the first day of data acquisition.

Table 26.1 Terra and Aqua MODIS VI product suites

Terra MODIS VI products	Aqua MODIS VI products
MOD13Q1: 16-day 250 m	MYD13Q1: 16-day 250 m
MOD13A1: 16-day 500 m	MYD13A1: 16-day 500 m
MOD13A2 16-day 1-km VI	MYD13A2 16-day 1-km VI
MOD13A3 monthly 1-km VI	MYD13A3 monthly 1-km VI
MOD13C1 16-day 0.05° VI	MYD13C1 16-day 0.05° VI
MOD13C2 monthly 0.05° VI	MYD13C2 monthly 0.05° VI

MOD09

Level-2 Corrected Surface
Reflectance

MOD09-L2G

Level 2 Gridded Corrected
Surface Reflectance

- 6 inputs -

MOD9GQK   = 250m Surface Reflectance
MOD09GHK   = 500m Surface Reflectance
MOD09GST   = 1km State Quality
Assurance
MODMGGAD   = 1km Viewing angles
MODPT0KM   = 250m Pointer Data

MOD13Q1/A1 ▼

Level 3 250m and 500m/16
days VI Product

MODPRAGG ▼

Level-3 Aggregated Surface
Reflectance

QA- CV- MVC
Temporal Compositing

MOD13C1

Level-3 0.05°(CMG)/16
days VI Product

MOD13A2

Level-3 1km/16 days VI
Product

Spatial Averaging

Temporal Averaging

MOD13C2

Level-3 0.05°
(CMG)/Monthly VI Product

MOD13A3

Level 3 1km/Monthly VI
Product

Fig. 26.1 Overview of the Terra MODIS-VI product suite and input dependencies

The MODIS VI product suite contains a set of output parameters known as science
datasets (SDS) for each composited, selected pixel, which include the following:
(1) composited NDVI and EVI, (2) NDVI/ EVI output quality, (3) reflectances in band
1 (620–670 nm), band 2 (841–876 nm), band 3 (459–479 nm), and band 7 (2,105–
2,155 nm), (4) sensor zenith view angle, solar zenith angle, and relative azimuth;
(5) day of year, which was added in the C5 product versions, and (6) pixel reliability.

The 500-m and 1-km VI product are computed from aggregated surface reflectances, while the climate modeling grid (CMG, 0.05° resolution) VI product is computed from the averaged reflectance values of good quality 1-km pixel, aggregated to 0.05° using a QA filter scheme that removes lower quality, cloud contaminated pixels. The aggregated CMG VI product includes the following: (1) NDVI and EVI, (2) NDVI and EVI standard deviations of the input 1-km pixel, (3) the number of QA-filtered pixels used to aggregate CMG pixels, and (4) the number of pixels within 30° sensor zenith angle in the CMG pixel.

26.3.1   Compositing Approach

Both the Terra and Aqua MODIS sensors provide nearly complete Earth coverage every day. Due to the ubiquitous presence of clouds and aerosols in daily global imaging sensors, *temporal compositing* of frequent measurements over set time intervals is used to remove clouds, aerosols, and cloud shadow contamination. The composited VIs are produced at 16-day interval from atmospherically corrected (MOD09), surface gridded reflectances with per pixel quality assurance (QA) information that were cloud-filtered. A constrained view angle, maximum value compositing (CV-MVC) method is used to select view angles to within ±30°. This is carried out with a per-pixel QA-based methodology that selects the closest to nadir value from the two or three highest NDVI values remaining after QA filtering lower quality pixels contaminated by residual clouds, shadows, high aerosol loadings, and large viewing geometries. The selected VI values represent actual, atmospherically corrected VI measurements at local solar zenith angle and close to nadir view geometries while retaining full traceability to the sensor acquisition.

This method is modified from the heritage AVHRR MVC methodology, which selects the highest NDVI value in a compositing cycle to best represent pixel greenness status (Holben 1986). Although maximum NDVI values greatly reduce clouds and aerosols, the highest NDVI value does not necessarily correspond to small sensor viewing angles or to the least-contaminated measurement. The reason stems from the bias resulting from the anisotropic properties of most vegetated surfaces wherein, off-nadir view angles in the forward scatter direction produce the highest NDVI values, even when contaminated by residual clouds and aerosols (Cihlar et al. 1994). With recent advances in atmosphere correction and sensor band-pass avoidance of water vapor and other absorbing gases, surface anisotropic influences are more pronounced and the highest NDVI is increasingly biased toward off-nadir pixel selection.

Potential value-added bidirectional reflectance distribution function (BRDF) applications to further reduce angular variations are possible with the view/sun angle information in the SDSs. For example, Los et al. (2005) adjusted AVHRR-NDVI time-series (Pathfinder AVHRR Land data) to a standard illumination and viewing geometry by applying MODIS-derived kernels, resulting in a 50–85% reduction in BRDF effects.

26.3.2   Dynamic Range of the VI Products

Figure 26.2 depicts the spatial and temporal dynamic range of the MODIS VIs
across a range of vegetation cover types, from hyperarid deserts to dense forests.
Important vegetation parameters used in climate and hydrological modeling, such
as the green vegetation fraction, Fg, are commonly derived through simple linear
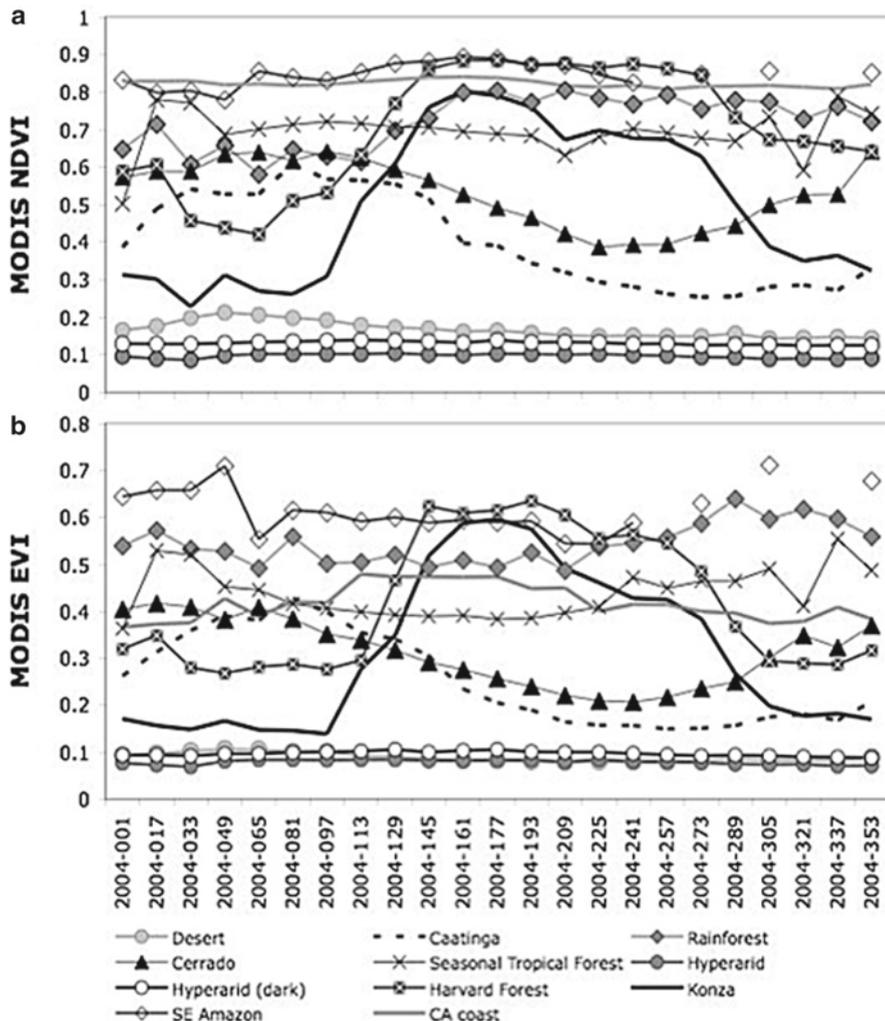combinations of high (vegetation) and low (soil) NDVI within a scene or biome.

Fig. 26.2 Representative MODIS VI seasonal profiles of major land cover types at 1-km resolu-
tion (MOD12A2), depicting dynamic ranges and values

In contrast to the AVHRR-NDVI dynamic range, $NDVI_{soil} = 0.04$ and $NDVI_{dense} = 0.52$ (Gutman and Ignatov 1998), MODIS-NDVI's dynamic range is much greater (NDVI ~0.1–0.90) due to narrower spectral bandwidths and more complete atmospheric correction (aerosols, water vapor) in the MODIS-NDVI product. The EVI values varied from 0.07 to ~0.7 for these same vegetation conditions at 1-km resolution. Several important differences exist between the NDVI- and EVI-based phenology profiles, particularly in the separation of needleleaf and broadleaf forests, the green-up and brown-down patterns of Harvard Forest and the Amazon, and the variation in background values associated with minimum greenness conditions. The EVI has sharper growing season peaks and is sensitive to canopy structure differences, while the NDVI appears more sensitive at the lower range of vegetation conditions while saturating in dense vegetation canopies (Fig. 26.2). The hyperarid desert baseline values are very stable, which suggest radiometrically calibrated bands through approximately 6 years of Terra-MODIS with no aging or degradation effects.

26.4 Validation and Accuracy of the VI Product Suite

The VI product attempts to retrieve cloud-free, near-nadir, top-of-canopy greenness at 16-day interval. Due to the global nature of the algorithm, some problems and uncertainties persist at local scales, mostly associated with residual clouds, shadows, aerosols, atmospheric correction performance, and view sun angle geometries, resulting in nonbiological artifacts and noise in the VI values. The accuracy of the VI product will vary in space and time due to geographical and seasonal variations in cloud persistence, unresolved clouds, the quality of upstream surface reflectance retrievals, sun angle, cross-band (red, NIR) spectral integrity, canopy background (soil, water, snow), topography, and geolocation (Huete and Liu 1994). For example, Miura et al. (2000) noted VI uncertainties due to sensor calibration of 0.01 and 0.02 for the NDVI and EVI, respectively.

Each MODIS VI measurement involves multiple, simultaneous variations in many of these noise sources, making it difficult to assess the influence of individual sources of uncertainty. The MODIS VI product, however, uses a set of QA classes, from best quality observations to fair quality data, to reduce *aggregate uncertainties* in VI values. The selection of the highest QA levels results in the highest confidence of cloud-free, low aerosol, and view angles within 30° of nadir with accuracies and precision within 0.03 and 0.02, respectively. As shown at the Jornada Experimental Range (Gao et al. 2003), VIs are readily computed from field-based, boom-mounted, and aircraft-borne instruments, and from a wide variety of fine and coarse space-based sensors, facilitating the comparison and radiometric validation of MODIS VIs. Light aircraft-mounted sensors, such as MODIS Quick-Airborne Looks (MQUALS), acquire nadir, top-of-canopy reflectance measurements from 150 to 500 m height, that greatly extend locally constrained field measurements to kilometer lengths to aid in validation (Huete et al. 1999).

26.4.1 Angular Sources of Uncertainty

Differences in anisotropic properties between red and NIR reflectances result in unique VI-dependent angular variations that require constraining in the composited VI products for more accurate analysis of vegetation dynamics, including landscape phenology. Fensholt et al. (2006) studied NDVI's dependence on solar and viewing geometries with MODIS and the Meteosat Second Generation (MSG) Spinning Enhanced Visible and Infrared Imager (SEVIRI) sensor. They found higher red reflectances relative to NIR under backscatter conditions, which cause observed NDVI to decrease. In the forward scatter direction, red reflectance data are much more strongly reduced due to shadowing from the highly absorbent vegetated canopies, resulting in higher NDVI. Whereas NDVI is biased positively in forward scatter view directions, the EVI responds more positively to backscatter (sunlit vegetation) view directions; however, since MODIS CV-MVC compositing is based on NDVI values, any positive bias present in NDVI pixel selection will result in a negative bias in EVI values, or underestimation of greenness. In a compositing study of MODIS and AVHRR daily data to map burned area over the Iberian Peninsula, Chuvieco et al. (2005) found the standard MODIS compositing procedure provided close to nadir observation angles and good spatial coherence, while the traditional MVC compositing criterion of maximizing NDVI values provided poor results. A comparison of the MODIS VI compositing algorithm with the heritage MVC technique over an Amazon tile shows significant reductions in view angle influences and improvements in the quality of pixel selection (Fig. 26.3).

An alternative method to assess how well view angle variations are constrained is to compare the VI product with VIs generated with the MODIS Nadir BRDF-Adjusted Reflectance (NBAR) products, MOD43B4 and MCD43A4, which are generated at 1-km/16-day and 500-m/8-day intervals, respectively (Schaaf et al. 2002) (Fig. 26.4). The NBAR product generates nadir reflectances through BRDF model inversions applied to seven or more good QA and cloud-free acquisitions within a 16-day composite cycle. Cross-plots of NBAR VI with the standard VI product over three vegetation types reveal fairly consistent values with relatively small view angle biases (Fig. 26.4b). The MODIS VI and NBAR products are produced at local solar zenith angle, and thus both contain latitudinal and seasonal sun angle influences. Notwithstanding the seasonal significance of the sun angle bias, it is less of a problem in interannual time-series data and trend analyses, provided there is no sensor orbital drift (Los et al. 2005).

26.4.2 Atmosphere and Clouds

The primary inputs to the MODIS compositing algorithm are atmospherically corrected surface reflectances (MOD09), which result in a more accurate and consistent VI product. However, residual effects and artifacts will invariably persist and aerosol miscorrections may occur with high aerosol pixels not corrected to the same
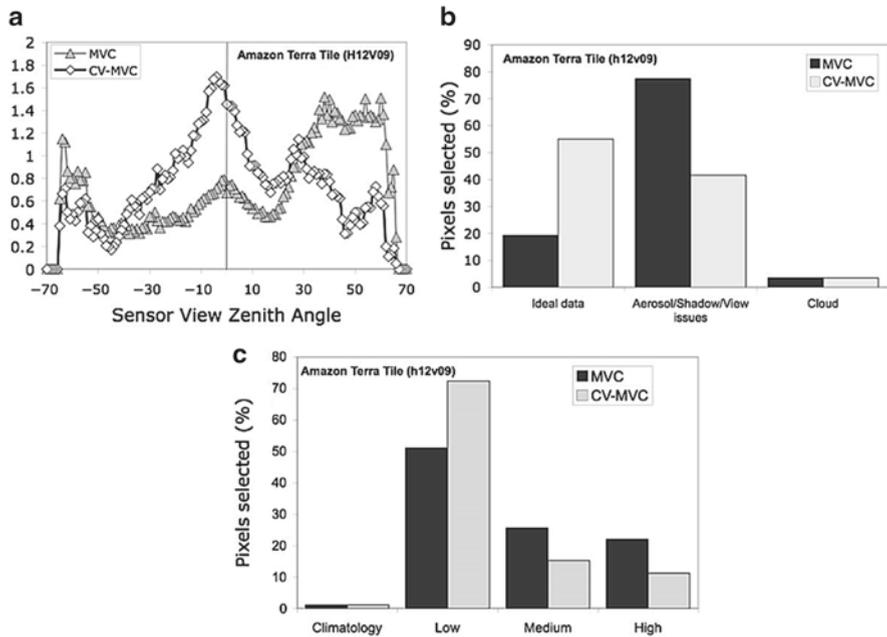
Fig. 26.3 Comparison of view angle distributions for pixels selected using MVC and CV-MVC methods for Amazon Tile (H12V09) (**a**), and resulting overall QA of output pixels (**b**), and for aerosol QA (**c**)

accuracy as low aerosol pixels. Furthermore, uncertainties exist in aerosol correction due to assumptions in the "dark object subtraction" and/or use of aerosol climatology as well as the use of aerosol input parameters at coarser (>10 km) resolution than the 250-m to 1-km VI pixel. Kaufman et al. (2005) found significant problems in aerosol correction attributed to residual cirrus and lower-level cloud contamination, and noted the difficulty of defining cloud contamination vs. aerosol growth. As a result, there likely are significant positive as well as negative error biases associated with atmospheric correction. An overcorrection of aerosols will result in abnormally low red reflectances and very high VI values, especially affecting the red-sensitive NDVI. The VIs are particularly sensitive to any disproportionate correction of the red and NIR bands. The inclusion of the blue band may improve or introduce more uncertainties in the EVI; however, the EVI was found to stabilize atmospheric aerosol effects in the Amazon (Miura et al. 2001) and Northern Asia (Xiao et al. 2003).

26.4.3 Biophysical Validation

An important aspect in validating VIs concerns their ability to capture essential biophysical phenomena with adequate fidelity and with minimal influences from the nongreen component of pixels (soil, nonphotosynthetic vegetation). Numerous
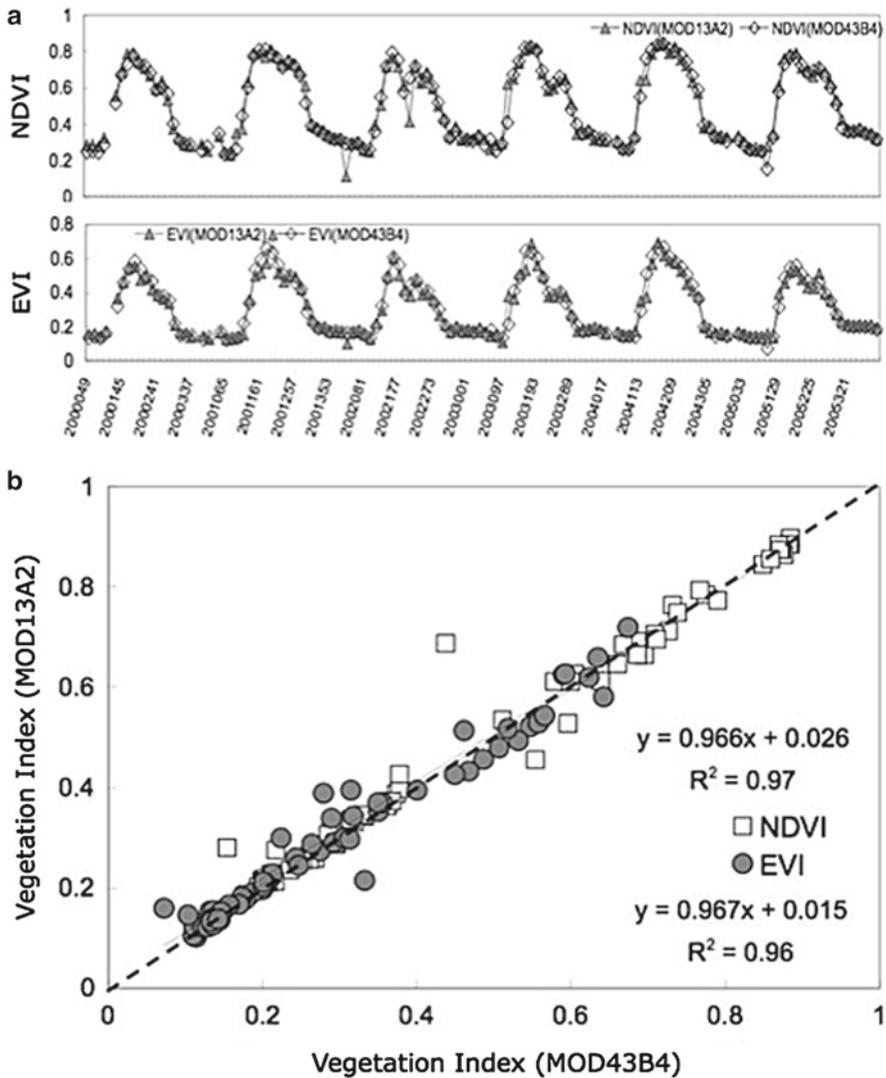
Fig. 26.4 Comparison of MODIS 1-km VI (MOD13A2) with 1-km NBAR generated VI (MOD43B4) for the Konza Prairie site, Kansas, United States over 6 years (**a**); and linear regression of MOD13A2 with MOD43B4 VIs for Konza Prairie, Lucky Hills shrub site in Arizona, and Harvard Forest in Massachusetts (**b**)

relationships between VIs and biophysical vegetation properties have been reported over the variable structural assemblages of chlorophyll, vegetation cover, and LAI per plant species or biome type. VI sensitivities and relationships are mostly based on empirical field measurements (Cohen et al. 2003) and canopy radiative transfer models (Huemmrich 2001). Using field-derived LAI values with higher resolution satellite

data, significant albeit nonlinear relationships were found between NDVI and EVI. For example, Chen et al. (2005) studied coniferous forest sites in Siberia with Landsat data. Poorer relationships are common when using coarser MODIS and SPOT-VGT Vis. For example, NDVI-LAI relationships in an European beech deciduous forest varied significantly over different phenology periods, with poor correlations during maximum LAI periods due to NDVI saturation (Wang et al. 2005). Cohen et al. (2003) also showed only weak correlations between field-measured LAI and several MODIS products, including VIs. However, LAI is very difficult to measure on the ground, particularly at scales consistent with MODIS measurements. Evidence shows that EVI enables extended sensitivity over higher LAI/biomass areas whereas the NDVI saturates (Fensholt 2004). Houborg and Soegaard (2004) found MODIS EVI was able to accurately describe the variation in green biomass in agricultural areas in Denmark, up to a maximum green LAI of 5 ($r^2 = 0.91$).

Conversely, the lack of a direct correspondence between VIs and canopy biophysical properties, such as LAI or Fg, does not compromise the utility of VIs in predicting biophysical processes such as photosynthesis or transpiration. Monteith and Unsworth (1990) noted that VIs are legitimately usable to estimate the rate of processes that depend on absorbed light, such as primary production and transpiration, whereas the relationship of LAI or Fg to absorb PAR is strongly nonlinear and depends on leaf architecture and spectral properties. Furthermore, photosynthesis and transpiration are not evenly distributed through the canopy, but are driven mainly by light absorbed by leaves (LAI) at the top of canopy.

Field- and MODIS-based NDVI have demonstrated linear relationships with fPAR across several biome types, and its integral over the growing season was correlated with ecosystem net primary production (NPP) (Asrar et al. 1984; Huemmrich et al. 2005). However, soil background variations introduce noise and uncertainty in NDVI-biophysical relationships on the same order of magnitude as atmospheric contamination (Choudhury 1987; Goward and Huemmrich 1992). Strong, soil-dependent discrepancies in fPAR–NDVI relationships are seen in which, NDVI linearly varies with fPAR in canopies with bright soil backgrounds, while the simple ratio (NIR/red) is linear with fPAR in canopies underlain with darker soil backgrounds (Sellers 1987), hence a nonlinear NDVI relationship with fPAR. The type of soil background not only alters VI-biophysical relationships but affects their degree of linearity with important consequences to scaling (Jiang et al. 2006).

The EVI has proven useful to estimate fPAR in vegetated canopies with relationships that are largely independent of soil background (Gao et al. 2000; Xiao et al. 2004). Zhang et al. (2005) used MODIS data and a coupled leaf-canopy radiative transfer model (PROSAIL-2) and showed significant differences between fPAR absorbed by a canopy (fPAR$_{canopy}$) and fPAR absorbed by leaf chlorophyll (fPAR$_{chl}$) in a broadleaf forest canopy, noting that only fPAR$_{chl}$ is used for photosynthesis and useful to quantify primary production. They found MODIS NDVI approximated fPAR$_{canopy}$, while EVI was closely coupled with fPAR$_{chl}$. This was also demonstrated by Xiao et al. (2004, 2005a) with MODIS seasonal analyses in both needleleaf and broadleaf forests, suggesting that EVI is probably more simply related to the chlorophyll content or *canopy greenness*.
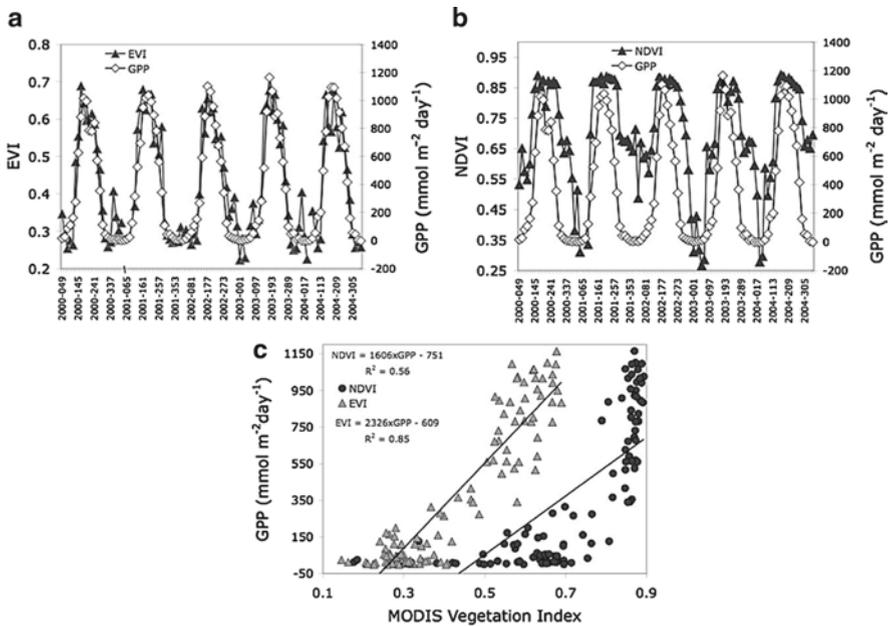
Fig. 26.5 MODIS EVI (**a**) and NDVI (**b**) comparisons with 16-day averaged tower flux measurements of gross primary productivity (GPP) for 5 years at Harvard Forest site (3 × 3 MOD13A2 pixels); and linear regression between MODIS VI and Tower GPP (**c**)

Rahman et al. (2005) and Sims et al. (2006) have shown how MODIS EVI and gross primary productivity (GPP) are highly correlated across a number of North American Ameriflux tower sites. An example of how well seasonal EVI tracks tower-calibrated GPP measurements of carbon fluxes at the Harvard Forest site is shown in Fig. 26.5. In the case of NDVI, there is some saturation and an overestimation of GPP, particularly after the peak growing season, a problem also observed with MODIS NDVI at the Sky Oaks savanna field site (Cheng et al. 2006). The use of tower flux measurements with remote sensing illustrates the power of integrating remote sensing and ground data. The generality of local, single-tower site studies may cast some doubts, and unexpected remote sensing observations are probably attributable to artifacts. For example, from a seasonal interference pattern induced by cloud cover, aerosol, or sun angle, the consistency between the independent VI and tower-derived flux observations lends confidence to both findings.

Each MODIS product revision generates improvements in product quality, and product uncertainties and accuracies are better characterized. To guide the user community in assessing the quality of individual MODIS products, various levels or stages of validation are defined (Morisette et al. 2002). The Collection 5 MODIS VI products are at stage 2 validation, i.e., their performance was assessed over a widely distributed set of locations and time periods with several in situ and validation efforts. The highest, stage 3 validation, will require complete and global product accuracy characterization in a systematic and statistically robust way.

26.5   Science and Applications

26.5.1   Carbon and Water Science

Recent applications of highly calibrated MODIS VIs have demonstrated their utility in studies of ecosystem functioning, which affect net ecosystem CO_2 exchange and water between land and the atmosphere. Huete et al. (2006a) found a strong, linear and consistent relationship between seasonal EVI and tower-cali-brated GPP measurements of carbon fluxes in both intact rainforest and forest conversion to pasture and agricultural sites in the Amazon, and suggested that basin-wide carbon fluxes are constrainable by integrating MODIS and local flux measurements. The EVI provides a more direct relationship than NDVI with photosynthesis in high-LAI Amazon forests by relying on the more sensitive NIR canopy reflectance, which is less prone to saturate. Theoretical analyses support this behavior and conclude that spectral indices, which are more functional with NIR best describe area-averaged canopy photosynthetic capacities and GPP (Sellers 1987).

The relationship strength between tower GPP fluxes and MODIS EVI is gener-ally highest in deciduous forests and lower for evergreen sites. However, the EVI is useful to estimate GPP with relatively high accuracy for most sites without direct consideration of light-use efficiency (LUE), thus simplifying carbon balance models over most vegetation types (Rahman et al. 2005; Sims et al. 2006). Yang et al. (2007) developed a continental-scale measure of GPP by integrating MODIS EVI and AmeriFlux data using support vector machines (SVMs).

Most carbon exchange models use a relationship in which LUE is derived and scaled down with available meteorological information, normally, at very coarse resolution. MODIS EVI data were incorporated into the Vegetation Photosynthesis Model to produce tower-calibrated predictions of GPP across a series of biomes, including evergreen and deciduous forest sites in temperate North America, and in seasonally moist tropical evergreen forests in the Amazon (Xiao et al. 2005a, b),

$$\text{GPP} = (\varepsilon_0 \times T \times W \times P) \times \text{fPAR}_{\text{PAV}} \times \text{PAR} \qquad (26.3)$$

where fPAR_{PAV} is derived from EVI and maximum LUE (ε_0) is reduced by the tem-perature (T), moisture (W), and phenology (P) scalars. NPP was modeled with monthly EVI inputs to the NASA-CASA (Carnegie Ames Stanford Approach) model, and closely resembled both the measured high- and low-seasonal carbon fluxes, enabling prediction of peak growing season uptake rates of CO_2 in irrigated croplands and moist temperate forests (Potter et al. 2007).

Combined remote sensing and in situ tower flux measurements have also yielded close relationships with water fluxes (Glenn et al. 2007). Yang et al. (2006) derived continental-scale estimates of evapotranspiration (ET) by combining MODIS data with eddy covariance flux tower measurements using an inductive machine learning technique called SVM. They found MODIS EVI the most important explan-atory factor in their fairly accurate ET estimates (root mean square of 0.62 mm/day).

At regional scales, ET measurements from nine flux towers established in riparian plant communities dominated by five major plant types on the Middle Rio Grande, Upper San Pedro River, and Lower Colorado River were found to correlate strongly with MODIS EVI values. The inclusion of maximum daily air temperatures (T_a) measured at the tower sites further improved this relationship ($r^2 = 0.74$) (Nagler et al. 2005a). ET measured at flux tower sites in semiarid riparian and upland grass and shrub plant communities were also strongly correlated with MODIS EVI ($r = 0.80$–0.94) (Nagler et al. 2005b). Examples of MODIS EVI-tower ET relationships at riparian and shrubland sites at the 2004 Soil Moisture Experiment (SMEX04) are depicted in Fig. 26.6. Seasonal EVI profiles track ET fairly well when transpiration
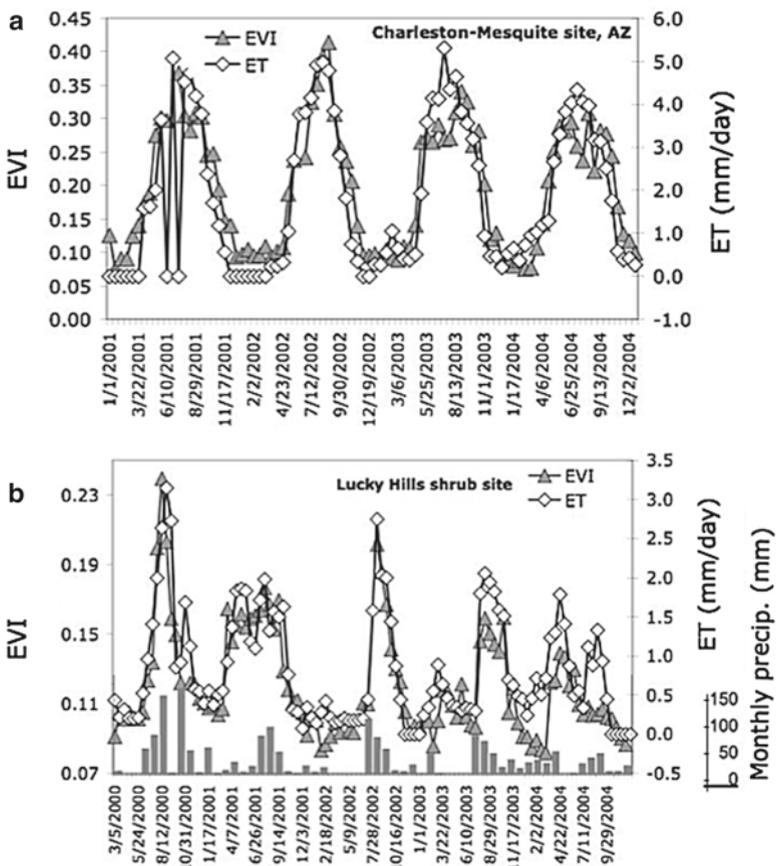
Fig. 26.6 MODIS EVI-eddy covariance tower ET relationships at riparian (**a**) and upland shrub (**b**) vegetation communities at the SMEX04 site in southeast Arizona, using MOD13Q1. The strong evaporation component in the upland shrub site during rain events results in significant departures from seasonal EVI values (tower flux data provided by Bill Emmerich and Russell Scott, USDA-ARS Southwest Watershed Research Center, Tucson, AZ)

dominates water fluxes, as found in the riparian site and during inter-storm periods in the upland shrub site with coarse, well-drained soils (Nagler et al. 2007).

The high direct correlation between VIs and GPP and ET in so many different ecosystems may seem surprising since, in theory, CO_2 and water exchanges are related not just to foliage density but to environmental variables (PAR, air temperature, vapor pressure deficit, wind), which can vary considerably over short time periods. However, according to the "resource optimization paradigm," plants tend to adjust their foliage density over time periods of days to weeks, to match the level of photosynthesis supportable by the environment (Field et al. 1995).

26.5.2   Phenology Studies

The VIs are widely used to characterize vegetation phenology (onset of greening and subsequent browning and dormancy), which is critical to understand ecosystem functioning and associated seasonal patterns of carbon, water, and energy fluxes (Reed et al. 2003). Phenology is also important to quantify ecosystem responses to climate variability, and in coupling land processes into global and regional climate models.

The extended sensitivity of the MODIS EVI has greatly facilitated phenology studies in dense tropical rainforests (Xiao et al. 2005b, 2006a). Using MODIS 250-m and CMG EVI, Huete et al. (2006a) were able to detect phenological variations in greenness, attributed to leaf flushing and leaf exchange, in densely vegetated Amazon tropical rainforests. They found rainforests to green-up by 25% in the dry season in response to the availability of sunlight, a finding confirmed by close couplings to tower-calibrated GPP measurements. Cleared forest areas, on the other hand, showed dry-season declines in EVI, presumably because the more shallow-rooted vegetation had reduced access to deep soil water. Ichii et al. (2007) further combined MODIS EVI with the BIOME-BGC (BioGeochemical Cycles) terrestrial ecosystem model to constrain spatial variability in rooting depths of forest trees over the Amazon and improve the assessments of carbon, water, and energy cycles in tropical forests. They simulated seasonal variations in GPP with different rooting depths (1, 3, 5, and 10 m) at local and regional scales and determined which rooting depths estimated GPP consistent with satellite-based observations. Hence, they were able to map rooting depths across the Amazon with satellite data (Ichii et al. 2007).

MODIS NDVI and EVI were used to characterize the phenology patterns and assess woody plant crown cover across a gradient of physiognomic vegetation classes in the Brazilian cerrado biome (Ratana et al. 2005). Kawamura et al. (2005) monitored short-term phenological changes in rangeland forage conditions with MODIS EVI in the semiarid Xilingol steppe in Inner Mongolia. They were able to estimate forage quantity and derive seasonal changes in live biomass and standing crude protein concentration over areas with different grazing intensities, useful to provide timing information for hay cutting based on nutritive value to

range managers. MODIS NDVI was successfully used to detect varying vegetation conditions caused by locust infestation, and provided a timely monitoring method for locust outbreaks in East China (Zha et al. 2005).

AVHRR-NDVI time-series analysis in high-latitude environments has demonstrated special difficulties due to the dominance of evergreen species with short growing seasons, and long periods of darkness with persistent snow cover in winter. Recently, however, Beck et al. (2006) applied double logistic functions to MODIS NDVI time-series data, and were able to estimate biophysical parameters related to the timing of spring and autumn phenology events in northern Scandinavia.

A MODIS-based algorithm was developed to generate timely and updated geospatial information on paddy rice distributions for irrigation, food security, trace gas emission estimates, and risk assessment of avian flu over South and Southeast Asia (Xiao et al. 2006b). Initial periods of flooding and the phenological growth patterns of paddy rice fields were assessed at regional scales with a three-index algorithm based on NDVI, EVI, and a Land Surface Water Index (Xiao et al. 2006b).

The MODIS vegetation phenology product (MOD12Q2) uses maximum inflections in seasonal NBAR-derived EVI profiles to produce a global set of phenology metrics based on key transition dates related to vegetation growth activity (Zhang et al. 2003). The NBAR-EVI was successfully used to map the phenology of single, double, and triple rice cropping patterns in the Mekong delta, where previously, this was only accomplished with SAR data (Sakamoto et al. 2005, 2006). The NBAR-EVI was also used to show the effect of urban climates on vegetation phenology transition dates in North American cities (Zhang et al. 2004). Strong heat island effects were found in urban areas with increases in the growing season of ~15 days and delays in the onset of dormancy, relative to adjacent nondisturbed ecosystems, a pattern that decays exponentially with distance from urban areas.

26.5.3 Societal Applications

The MODIS VI data are routinely assimilated in a wide variety of different applications, including agriculture, natural resource monitoring and forecasting systems, invasive species, pest and famine early warning systems (FEWS), and diseases in support of scientific and societal purposes. Several priority national application areas, such as agricultural efficiency, carbon management, disaster management, ecological management, homeland security, invasive species, public health and water management, assimilate MODIS VIs as part of their decision support tools of value and benefit to resource management, policy decisions, and resource exploration (NASA 2008).

The MODIS NDVI data are used in interactive monitoring tools for FEWS (USAID 2008), and are assimilated into decision support systems operated by the Production Estimates and Crop Assessment Division (PECAD) of the Foreign Agricultural Service (USDA-FAS) to disseminate global crop conditions and

agricultural production information for selected commodities at a global scale. The MODIS VI product is shared online through Cropexplorer (USDA 2008). The Upper Midwest Aerospace Consortium provides MODIS NDVI data to farmers, ranchers, and foresters living in remote areas of the Upper Midwest, land managers from the Native American Community, and Federal and State Agencies (Seelan et al. 2003; UMAC 2008).

An increasing number of natural resource managers are using Web-based geospatial decision support tools that integrate time-series of both historical and current NDVI data derived from multiple sensors to make better informed planning and management decisions (van Leeuwen et al. 2006). MODIS VI data was used in an operational module, "Integrated Warning Deforestation System for the Amazon" (SIAD), an initiative of the Brazilian government within the scope of the Amazon Protection System (SIPAM) (Ferreira et al. 2007). Jin and Sader (2005) investigated the utility of MODIS NDVI and reflectance products to detect and quantify forest disturbances in northern Maine. MODIS VIs are also utilized as part of the Invasive Species Forecasting System (ISFS), a successful partnership between multilevel agencies (USGS and NASA), academic institutions, and private organizations with the aim of monitoring the introduction and dissemination of invasive species (USGS ISFS 2008). MODIS NDVI time-series are used to predict potential invasive species habitats, so that control or preventative measures are applied before irreversible changes occur (Schnase et al. 2002). Using MODIS NDVI, Franklin et al. (2006) studied the negative impacts of an invasive African grass species, buffelgrass (*Pennisetum ciliare*), on diversity of native rangeland plant communities in Sonora, Mexico.

MODIS VIs contribute to carbon sequestration programs such as the Web-based interface (CASA-CQUEST Carbon Query and Evaluation Support Tools; NASA CASA 2008) to inform land managers about carbon management and sequestration potential. Time-series MODIS VI images are also used for epidemiological purposes (infectious and vector-borne diseases) to address many environment-related health problems by visualizing regions that are either greener (wetter) than average or less green (drier) than normal to aid in assessing outbreaks of Malaria, Rift Valley fever, and other mosquito-borne diseases (Beck et al. 2000).

26.6   Vegetation Index Continuity and Long-Term Data Records

The continuous monitoring of Earth's vegetation benefits from numerous operational satellite instruments that exist today. Their output is potentially useful to generate a seamless, long-term data record for global change studies. The MODIS VI products will play an important role in extending VI observations from previous AVHRR sensors, and bridge a VI data record into the follow-on operational sensor, the Visible Infrared Imaging Radiometer Suite (VIIRS) slated for launch as part of the National Polar Orbiting Environmental Sensor System (NPOESS) Preparatory

Project (NPP) (Fig. 26.7). The MODIS and VIIRS sensors have similar bandwidths in the red (620–670 and 600–680 nm, respectively) and NIR (841–876 and 845–884 nm, respectively) portions of the spectrum, but differ in their blue channels (459–479 and 478–498 nm, respectively), which may present problems with EVI continuity (Huete et al. 2006b). The VIIRS pixel size is coarser than MODIS (375 m vs. 250 m in the red and NIR) but finer than AVHRR (1.1 km). The bandwidths of both sensors vary considerably from those of the AVHRR, which may present challenges in data continuity and fusion. A greater sensitivity and dynamic range of MODIS-NDVI in comparison with AVHRR-NDVI are known and attributed to the higher spatial resolutions, and narrower red and NIR spectral bandwidths of MODIS, which avoid atmospheric water vapor influences (Huete et al. 2002; Fensholt 2004; van Leeuwen et al. 2006; Miura et al. 2006; Gallo et al. 2005). In a study of NDVI–LAI relationships with NOAA-14 AVHRR, SPOT-4 VGT, and Terra MODIS data, Wang et al. (2005) found significant differences in slope, intercept, and strength of relationships.

However, recent operational water vapor corrections applied to AVHRR/3 data and the narrower bandwidth of AVHRR/3 channel-1 have resulted in near 1:1 linear relationships in 1-km NDVI value derived from overlapping time periods of NOAA-16 and -17 AVHRR/3, and Terra and Aqua MODIS sensors (Gallo et al. 2004, 2005). This suggests that the feasibility to reprocess historical AVHRR datasets to provide continuity of NDVI through the NPOESS era. Brown et al. (2006) demonstrated the consistency of long-term NDVI time-series derived from AVHRR, SPOT-VGT, SeaWiFS, and MODIS sensors. MODIS VI data from Terra and Aqua were shown as interchangeable, despite their overpass time differences (10:30 h vs. 13:30 h) (Gallo et al. 2005). As a result, a MODIS "combined" Terra+Aqua VI product that improves temporal compositing frequency from 16 to 8 days was accomplished in Collection 5, by offsetting the Aqua 16-day composite with an 8-day phase difference so that the two products are merged to generate VIs that are 8 days apart.
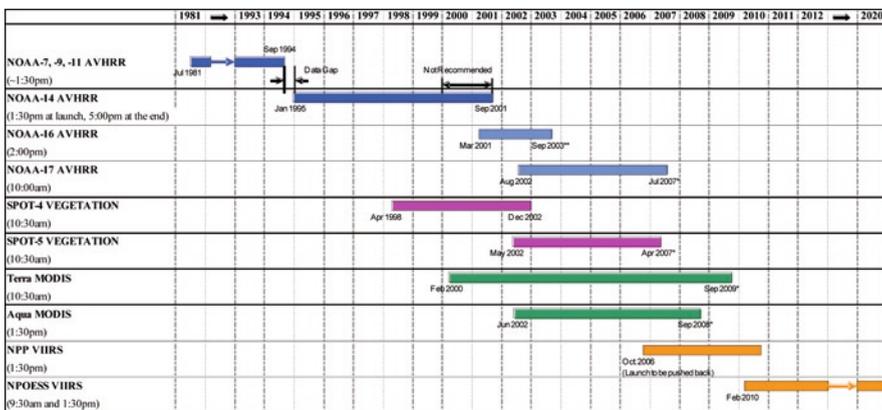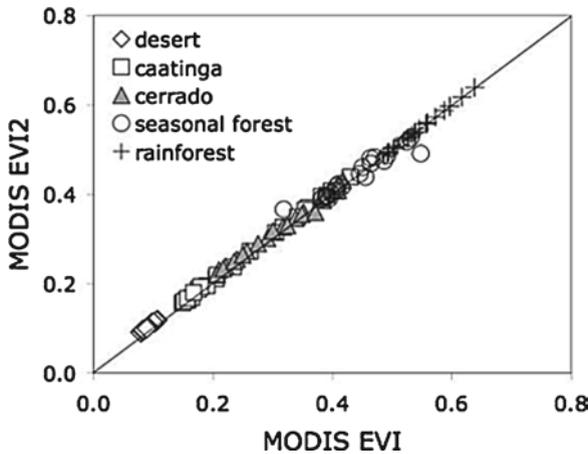

Fig. 26.7 Role of Terra- and Aqua-MODIS sensors within the long-term VI time-series data record

Fig. 26.8 Regression of standard EVI product (MOD13A2) with the two-band EVI2 version for various sites in South America

A backward compatibility of the EVI to the historical AVHRR record to complement the NDVI is also feasible. The EVI uses a blue band to minimize residual atmospheric effects, however, a two-band SAVI-like version is definable when the "blue band" is unavailable, as follows (Jiang et al. 2008):

$$EVI2 = 2.5(\rho_{NIR} - \rho_{red}) / (1 + \rho_{NIR} + 2.4\rho_{red}) \tag{26.4}$$

Although the EVI2 is computed without a blue band, it remains functionally equivalent to the EVI, although slightly more prone to aerosol noise, which may become less significant with continuing advancements in atmosphere correction (Fig. 26.8). Currently, the EVI2 is used as a backup equation in the MODIS EVI product when snow cover problems render the product unstable. Yoshioka et al. (2003) developed a "bottom-to-top" approach to translate the NDVI from one sensor to another, whereby vegetation isoline equations originally developed to model the behavior of red vs. NIR reflectances were applied to red vs. red and NIR vs. NIR reflectances between two sensors. This theoretical approach provided a better mechanistic understanding and predictive modeling of cross-sensor relationships for the NDVI and input reflectances as well as other VIs, such as EVI.

26.7   Conclusions

Since the respective launches of the Terra and Aqua platforms, MODIS VI products have provided highly calibrated and frequent global measurements of the land surface for monitoring of vegetation dynamics, landscape phenology, and productivity. As outlined in this chapter, new advances in earth system science and in operational applications of satellite data continue with the MODIS VI products. In contrast to

previous satellite observations with AVHRR-NDVI, the MODIS VI products are generated at higher spatial resolution and with negligible water vapor influences and lower-cloud and aerosol contamination. Furthermore, a second index, EVI, offers extended sensitivity into high biomass/LAI canopies, and has provided stronger relationships with canopy biophysical processes, such as photosynthesis and transpiration. The two VIs complement each other and offer a more complete characterization of the entire range of surface biophysical/chemical information and processes taking place in vegetated canopies. Although, the literature has thus far shown the strong utility of both MODIS NDVI and EVI, further research and consensus are valuable in resolving specific VI relationships with canopy properties (chlorophyll content, fPAR, LAI, Fg) and biophysical processes (photosynthesis and transpiration). This will facilitate their inputs to biogeochemical, hydrological, and productivity models, and allow derivation of on-demand biophysical products from the VI data record.

Much of the success in the operational use of VIs resides in their simplicity and ready fusion with data from other sensor systems and platforms. VIs are easily measured on the ground and field-derived biophysical relationships are scaled through finer-grained satellite data or directly to MODIS resolutions. The MODIS VIs are an integral component in the continuing development of long-term time-series applications and climate data records; the proposed AVHRR/MODIS/VIIRS satellite time-series will provide a critical long-term VI data record for Earth studies.

References

Asrar G, Fuchs M, Kanemasu ET, Hatfield SL (1984) Estimating absorbed photosynthetic radiation and leaf area index from spectral reflectance in wheat. Agron J 76:300–306

Beck LR, Lobitz BM, Wood BL (2000) Remote sensing and human health: new sensors and new opportunities. Emerg Infect Dis 6:217–227

Beck PSA, Atzberger C, Høgda KA, Johansen B, Skidmore AK (2006) Improved monitoring of vegetation dynamics at very high latitudes: A new method using MODIS NDVI. Remote Sens Environ 100:321–334

Brown ME, Pinzon JE, Didan K, Morisette JT, Tucker CJ (2006) Evaluation of the consistency of long-term NDVI time series derived from AVHRR, SPOT-Vegetation, SeaWiFS, MODIS, and Landsat ETM+ sensors. IEEE Trans Geosci Remote Sens 44:1787–1793

Chen X, Vierling L, Deering D, Conley A (2005) Monitoring boreal forest leaf area index across a Siberian burn chronosequence: a MODIS validation study. Int J Remote Sens 26:5433–5451

Cheng Y, Gamon JA, Fuentes DA, Mao Z, Sims DA, Qiu H, Claudio H, Huete A, Rahman AF (2006) A multi-scale analysis of dynamic optical signals in a Southern California chaparral ecosystem: a comparison of field, AVIRIS and MODIS data. Remote Sens Environ 103:369–378

Choudhury BJ (1987) Relationships between vegetation indices, radiation absorption, and net photosynthesis evaluated by a sensitivity analysis. Remote Sens Environ 22:209–233

Chuvieco E, Ventura G, Martin MP, Gomez I (2005) Assessment of multitemporal compositing techniques of MODIS and AVHRR images for burned land mapping. Remote Sens Environ 94:450–462

Cihlar J, Manak D, Voisin N (1994) AVHRR bidirectional reflectance effects and compositing. Remote Sens Environ 48:77–88

Cohen WB, Maiersperger TK, Yang Z, Gower ST, Turner DP, Ritts WD, Berterretche M, Running SW (2003) Comparisons of land cover and LAI estimates derived from ETM+ and MODIS for four sites in North America: a quality assessment of 2000/2001 provisional MODIS products. Remote Sens Environ 88:233–255

Fensholt R (2004) Earth observation of vegetation status in the Sahelian and Sudanian West Africa: comparison of terra MODIS and NOAA AVHRR satellite data. Int J Remote Sens 25:1641–1659

Fensholt R, Sandholt I, Stisen S, Tucker C (2006) Analysing NDVI for the African continent using the geostationary Meteosat second generation SEVIRI sensor. Remote Sens Environ 101:212–229

Ferreira NC, Ferreira LG, Huete AR, Ferreira ME (2007) An operational deforestation mapping system using MODIS data and spatial context analysis. Int J Remote Sens 28:47–62

Field CB, Randerson JT, Malmstrom CM (1995) Global net primary production: combining ecology and remote sensing. Remote Sens Environ 51:74–88

Franklin KA, Lyons K, Nagler PL, Lampkin D, Glenn EP, Molina-Freaner F, Markow T, Huete AR (2006) Buffelgrass (*Pennisetum ciliare*) land conversion and productivity in the plains of Sonora, Mexico. Biol Conserv 127:62–71

Gallo KP, Eidenshink JC (1988) Differences in visible and near-IR responses, and derived vegetation indices, for the NOAA-9 and NOAA-10 AVHRRs: a case study. Photogramm Eng Remote Sens 54:485–490

Gallo K, Ji L, Reed B, Dwyer J, Eidenshink J (2004) Comparison of MODIS and AVHRR 16-day normalized difference vegetation index composite data. Geophys Res Lett 31:L07502. doi:10.1029/2003GL019385

Gallo K, Ji L, Reed B, Eidenshink J, Dwyer J (2005) Multi-platform comparisons of MODIS and AVHRR normalized difference vegetation index data. Remote Sens Environ 99:221–231

Gao X, Huete AR, Ni W, Miura T (2000) Optical-biophysical relationships of vegetation spectra without background contamination. Remote Sens Environ 74:609–620

Gao X, Huete AR, Didan K (2003) Multisensor comparisons and validation of MODIS vegetation indices at the semiarid Jornada Experimental Range. IEEE Trans Geosci Remote Sens 41:2368–2381

Glenn EP, Huete AR, Nagler PL, Hirschboeck KK, Brown P (2007) Integrating remote sensing and ground methods to estimate evapotranspiration. CRC Crit Rev Plant Sci 26:139–168

Gobron N, Pinty B, Verstraete MM, Widlowski JL (2000) Advanced vegetation indices optimized for up-coming sensors: design, performance, and applications. IEEE Trans Geosci Remote Sens 38:2489–2505

Goward SN, Huemmrich KF (1992) Vegetation canopy PAR absorptance and the normalized difference vegetation index: an assessment using the SAIL model. Remote Sens Environ 39:119–140

Gutman G, Ignatov A (1998) The derivation of the green vegetation fraction from NOAA/AVHRR data for use in numerical weather prediction models. Int J Remote Sens 19:1533–1543

Holben BN (1986) Characteristics of maximum-value composite images from temporal AVHRR data. Int J Remote Sens 7:1417–1434

Houborg RM, Soegaard H (2004) Regional simulation of ecosystem CO_2 and water vapor exchange for agricultural land using NOAA AVHRR and Terra MODIS satellite data. Application to Zealand, Denmark. Remote Sens Environ 93:150–167

Huemmrich KF (2001) The GeoSail model: a simple addition to the SAIL model to describe discontinuous canopy reflectance. Remote Sens Environ 75:423–431

Huemmrich KF, Privette JL, Mukelabai M, Myneni RB, Knyazikhin Y (2005) Time series validation of MODIS land biophysical products in a Kalahari woodland, Africa. Int J Remote Sens 26:4381–4398

Huete AR (1988) A soil-adjusted vegetation index (SAVI). Remote Sens Environ 25:295–309

Huete AR (1989) Soil influences in remotely sensed vegetation canopy spectra. In: Asrar G (ed) Theory and applications of optical remote sensing. Wiley, New York, pp 107–141

Huete AR, Liu H (1994) An error and sensitivity analysis of the atmospheric- and soil-correcting variants of the NDVI for MODIS-EOS. IEEE Trans Geosci Remote Sens 32:897–905

Huete A, Keita F, Thomé K, Privette J, van Leeuwen WJD, Justice C, Morisette J (1999) A light aircraft radiometric package for MODLAND quick airborne looks (MQUALS). Earth Obs 11:22

Huete A, Didan K, Miura T, Rodriguez EP, Gao X, Ferreira LG (2002) Overview of the radiometric and biophysical performance of the MODIS vegetation indices. Remote Sens Environ 83:195–213

Huete AR, Didan K, Shimabukuro YE, Ratana P, Saleska SR, Hutyra LR, Yang W, Nemani RR, Myneni R (2006a) Amazon rainforests green-up with sunlight in dry season. Geophys Res Lett 33:L06405. doi:10.1029/2005GL025583

Huete AR, Miura T, Kim Y, Didan K, Privette J (2006b) Assessments of multisensor vegetation index dependencies with hyperspectral and tower flux data. In: SPIE proceedings on remote sensing and modeling of ecosystems for sustainability III, vol 6298-45, San Diego, CA

Ichii K, Hashimoto H, White MA, Potter C, Hutyra LR, Huete AR, Myneni RB, Nemani RR (2007) Constraining rooting depths in tropical rainforests using satellite data and ecosystem modeling for accurate simulation of gross primary production seasonality. Global Chang Biol 13:67–77

Jiang Z, Huete AR, Chen J, Chen Y, Li J, Yan G, Zhang X (2006) Analysis of NDVI and scaled difference vegetation index retrievals of vegetation fraction. Remote Sens Environ 101:366–378

Jiang Z, Huete AR, Didan K, Miura T (2008) Development of a 2-band enhanced vegetation index without a blue band. Remote Sens Environ 112:3833–3845

Jin S, Sader SA (2005) MODIS time-series imagery for forest disturbance detection and quantification of patch size effects. Remote Sens Environ 99:462–470

Kaufman Y, Tanré D (1992) Atmospherically resistant vegetation index (ARVI) for EOS-MODIS. IEEE Trans Geosci Remote Sens 30:261–270

Kaufman YJ, Remer LA, Tanre D, Li R, Kleidman R, Mattoo S, Levy RC, Eck TF, Holben BN, Ichoku C, Martins JV, Koren I (2005) A critical examination of the residual cloud contamination and diurnal sampling effects on MODIS estimates of aerosol over ocean. IEEE Trans Geosci Remote Sens 43:2886–2897

Kawamura K, Akiyama T, Yokota H, Tsutsumi M, Yasuda T, Watanabe O, Wang G, Wang S (2005) Monitoring of forage conditions with MODIS imagery in the Xilingol steppe, Inner Mongolia. Int J Remote Sens 26:1423–1436

Liu H, Huete A (1995) A feedback based modification of the NDVI to minimize canopy background and atmospheric noise. IEEE Trans Geosci Remote Sens 33:457–465

Los SO, North PRJ, Grey WMF, Barnsley MJ (2005) A method to convert AVHRR normalized difference vegetation index time series to a standard viewing and illumination geometry. Remote Sens Environ 99:400–411

Miura T, Huete A, van Leeuwen WJD, Didan K (1998) Vegetation detection through smoke-filled AVIRIS images: an assessment using MODIS band passes. J Geophys Res 103:32001–32011

Miura T, Huete AR, Yoshioka H (2000) Evaluation of sensor calibration uncertainties on vegetation indices for MODIS. IEEE Trans Geosci Remote Sens 38:1399–1409

Miura T, Huete AR, Yoshioka H, Holben BN (2001) An error and sensitivity analysis of atmospheric resistant vegetation indices derived from dark target-based atmospheric correction. Remote Sens Environ 78:284–298

Miura T, Huete A, Yoshioka H (2006) An empirical investigation of cross-sensor relationships of NDVI and red/near-infrared reflectance using EO-1 Hyperion data. Remote Sens Environ 100:223–236

Monteith JL, Unsworth MH (1990) Principles of environmental physics, 2nd edn, Arnold, London

Morisette JT, Privette JL, Justice CO (2002) A framework for the validation of MODIS Land products. Remote Sens Environ 83:77–96

Myneni RB, Keeling CD, Tucker CJ, Asrar G, Nemani RR (1997) Increased plant growth in the northern high latitudes from 1981 to 1991. Nature 386:698–702

Nagler PL, Scott RL, Westenburg C, Cleverly JR, Glenn EP, Huete AR (2005a) Evapotranspiration on western U.S. rivers estimated using the enhanced vegetation index from MODIS and data from eddy covariance and Bowen ratio flux towers. Remote Sens Environ 97:337–353

Nagler PL, Cleverly J, Glenn E, Lampkin D, Huete A, Wan Z (2005b) Predicting riparian evapotranspiration from MODIS vegetation indices and meteorological data. Remote Sens Environ 94:17–35

Nagler PL, Glenn EP, Kim H, Emmerich W, Scott RL, Huxman TE, Huete AR (2007) Relationship between evapotranspiration and precipitation pulses in a semiarid rangeland estimated by moisture flux towers and MODIS vegetation indices. J Arid Environ 70:443–462

NASA CASA Project (2008) http://geo.arc.nasa.gov/sge/casa/cquestwebsite/index.html Accessed 27 Feb 2008

NASA Science Mission Directorate (2008) http://science.hq.nasa.gov/earth-sun/applications Accessed 27 Feb 2008

Potter C, Klooster S, Huete A, Genovese V (2007) Terrestrial carbon sinks for the United States predicted from MODIS satellite data and ecosystem modeling. Earth Interact 11:1–21

Rahman AF, Sims DA, Cordova VD, El-Masri BZ (2005) Potential of MODIS EVI and surface temperature for directly estimating per-pixel ecosystem C fluxes. Geophys Res Lett 32:L19404. doi:10.1029/2005GL024127

Ratana P, Huete AR, Ferreira L (2005) Analysis of cerrado physiognomies and conversion in the MODIS seasonal-temporal domain. Earth Interact 8:1–22

Reed BC, White M, Brown JF 2003. Remote sensing phenology. In: Schwartz MD (ed) Phenology: an integrative environmental science, Tasks for vegetation science, vol 39. Kluwer, Dordrecht, The Netherlands, p 569

Sakamoto T, Yokozawa M, Toritani H, Shibayama M, Ishitsuka N, Ohno H (2005) A crop phenology detection method using time-series MODIS data. Remote Sens Environ 96:366–374

Sakamoto T, Van Nguyen N, Ohno H, Ishitsuka N, Yokozawa M (2006) Spatio-temporal distribution of rice phenology and cropping systems in the Mekong Delta with special reference to the seasonal water flow of the Mekong and Bassac rivers. Remote Sens Environ 100:1–16

Schaaf CB, Gao F, Strahler AH, Lucht W, Li X, Tsang T, Strugnell NC, Zhang X, Jin Y, Muller J-P (2002) First operational BRDF, albedo nadir reflectance products from MODIS. Remote Sens Environ 83:135–148

Schnase JL, Stohlgren TJ, Smith JA (2002) The National Invasive Species Forecasting System: a strategic NASA/USGS partnership to manage biological invasions. Earth Observing Magazine August 2002:46–49

Seelan SK, Laguette S, Casady GM, Seielstad GA (2003) Remote sensing applications for precision agriculture: a learning community approach. Remote Sens Environ 88:157–169

Sellers PJ (1987) Canopy reflectance, photosynthesis, and transpiration. II. The role of biophysics in the linearity of their interdependence. Remote Sens Environ 21:143–183

Sims DA, Rahman AF, Cordova VD, El-Masri BZ, Baldocchi DD, Flanagan LB, Goldstein AH, Hollinger DY, Misson L, Monson RK, Oechel WC, Schmid HP, Wofsy SC, Xu L (2006) On the use of MODIS EVI to assess gross primary productivity of North American ecosystems. J Geophys Res 111:G04015. doi:10.1029/2006JG000162

Tucker CJ (1979) Red and photographic infrared linear combinations for monitoring vegetation. Remote Sens Environ 8:127–150

Tucker CJ, Pinzon JE, Brown ME, Slayback DA, Pak EW, Mahoney R, Vermote EF, El Saleous N (2005) An extended AVHRR 8-km NDVI dataset compatible with MODIS and SPOT vegetation NDVI data. Int J Remote Sens 26:4485–4498

Upper Midwest Aerospace Consortium (2008) http://www.umac.org/content/umac/about.shtml Accessed 27 Feb 2008

USAID Famine Early Warning Systems (2008) http://www.fews.net. Accessed 27 Feb 2008

Foreign Agriculture Service USDA (2008) Crop explorer. http://www.pecad.fas.usda.gov/cropexplorer/ Accessed 27 Feb 2008

USGS Invasive Species Forecasting System (2008) http://isfs.gsfc.nasa.gov Accessed 27 Feb 2008

van Leeuwen WJD, Orr BJ, Marsh SE, Herrmann SM (2006) Multi-sensor NDVI data continuity: uncertainties and implications for vegetation monitoring applications. Remote Sens Environ 100:67–81

Wang Q, Adiku S, Tenhunen J, Granier A (2005) On the relationship of NDVI with leaf area index in a deciduous forest site. Remote Sens Environ 94:244–255

Xiao X, Braswell B, Zhang Q, Boles S, Frolking S, Moore B III (2003) Sensitivity of vegetation indices to atmospheric aerosols: continental-scale observations in Northern Asia. Remote Sens Environ 84:385–392

Xiao X, Zhang Q, Braswell B, Urbanski S, Boles S, Wofsy S, Moore B III, Ojima D (2004) Modeling gross primary production of temperate deciduous broadleaf forest using satellite images and climate data. Remote Sens Environ 91:256–270

Xiao XM, Zhang QY, Hollinger D, Aber J, Moore B III (2005a) Modeling gross primary production of an evergreen needleleaf forest using MODIS and climate data. Ecol Appl 15:954–969

Xiao X, Zhang Q, Saleska S, Hutyra L, De Camargo P, Wofsy S, Frolking S, Boles S, Keller M, Moore B III (2005b) Satellite-based modeling of gross primary production in a seasonally moist tropical evergreen forest. Remote Sens Environ 94:105–122

Xiao X, Hagen S, Zhang Q, Keller M, Moore B III (2006a) Detecting leaf phenology of seasonally moist tropical forests in South America with multi-temporal MODIS images. Remote Sens Environ 103:465–473

Xiao X, Boles S, Frolking S, Li C, Babu JY, Salas W, Moore B III (2006b) Mapping paddy rice agriculture in south and Southeast Asia using multi-temporal MODIS images. Remote Sens Environ 100:95–113

Yang F, White MA, Michaelis AR, Ichii K, Hashimoto H, Votava P, Zhu AX, Nemani RR (2006) Prediction of continental-scale evapotranspiration by combining MODIS and AmeriFlux data through support vector machine. IEEE Trans Geosci Remote Sens 44:3452–3461

Yang F, Ichii K, White MA, Hashimoto H, Michaelis AR, Votava P, Zhu AX, Huete A, Running SW, Nemani RR (2007) Developing a continental-scale measure of gross primary production by combining MODIS and AmeriFlux data through support vector machine approach. Remote Sens Environ 110:109–122

Yoshioka H, Miura T, Huete AR (2003) An isoline-based translation technique of spectral vegetation index using EO-1 Hyperion data. IEEE Trans Geosci Remote Sens 41:1363–1372

Zha Y, Gao J, Ni S, Shen N (2005) Temporal filtering of successive MODIS data in monitoring a locust outbreak. Int J Remote Sens 26:5665–5674

Zhang X, Friedl MA, Schaaf CB, Strahler AH, Hodges JCF, Gao F, Reed BC, Huete A (2003) Monitoring vegetation phenology using MODIS. Remote Sens Environ 84:471–475

Zhang X, Friedl MA, Schaaf CB, Strahler AH, Schneider A (2004) The footprint of urban climates on vegetation phenology. Geophys Res Lett 31:L12209. doi:10.1029/2004GL020137

Zhang Q, Xiao X, Braswell B, Linder E, Baret F, Moore B III (2005) Estimating light absorption by chlorophyll, leaf and canopy in a deciduous broadleaf forest using MODIS data and a radiative transfer model. Remote Sens Environ 99:357–371